The measurement of poloidal magnetic field in a Tokamak by the change of polarization of an electromagnetic wave

1978 Plasma Phys. 20 295

(http://iopscience.iop.org/0032-1028/20/4/001)

Plasma Physics, Vol. 20, pp. 295 to 307
0032-1028/78/0401-0295$02.00/0

THE MEASUREMENT OF POLOIDAL MAGNETIC FIELD IN A TOKAMAK BY THE CHANGE OF POLARIZATION OF AN ELECTROMAGNETIC WAVE

S. E. SEGRE
Associazione Euratom–CNEN sulla Fusione, Centro Gas Ionizzati, Frascati, Italy

(*Received* 2 *May* 1977)

Abstract—This paper contains a theoretical development of a proposal for measuring the current distribution in a Tokamak from the change of polarization of an electromagnetic wave traversing the plasma. A simple numerical method is given for calculating the resulting polarization and is illustrated by examples. The effect of the radial variation of toroidal field is discussed. The analytic solution in the form of a series is used to obtain some properties of the output polarization.

1. INTRODUCTION

THE DISTRIBUTION of current density or equivalently of poloidal magnetic field in a Tokamak is of prime importance and various methods for measuring it have been proposed, however none is yet a standard method. A brief survey is given by CRAIG (1976).

A method involving the measurement of the change in polarization of an electromagnetic wave propagating across the plasma was proposed by DE MARCO and SEGRE (1972) and further developed by CRAIG. In the former paper which will henceforth be denoted as I, the polarization vector was used to describe the state of polarization and a differential equation was derived for the evolution of the polarization. It was found that when the change in polarization is small, the equation can be integrated analytically and an approximate expression for the output polarization as a function of plasma parameters is obtained. This analytic expression can then be inverted (by a generalized Abel inversion) to give the current density distribution $j(r)$ explicitly.

CRAIG (1976) has given a numerical method, valid also when the change in polarization is not small, which can be used to compute the output polarization for different assumed current density profiles. By means of a best fit to the measured polarization $j(r)$ can be determined.

In the present paper the analysis of I is extended in two directions. First in Section 3 it is shown that the differential equation can be used with advantage for a numerical solution which is simple and gives an accurate answer also for large polarization changes. Using this numerical method it is shown in Section 4 that the output polarization depends also on the sign of both the poloidal and toroidal magnetic fields, when polarization changes are not small. Secondly an exact analytic expression for the output polarization is given in Section 5 in the form of a series. This is used for an analytic discussion of the conditions required for the determination of $n(r)$ as proposed by Craig.

The simplicity of the numerical method derived in Section 3 recommends it for the analysis of future experimental results when many computations will be required.

2. CHANGE OF POLARIZATION FOR PROPAGATION IN A NON-UNIFORM PLASMA WITH MAGNETIC FIELD SHEAR

As in paper I we shall describe the state of polarization of a plane electromagnetic wave by means of the angles ψ, χ or the parameters s_1, s_2, s_3 as follows. For a wave propagating in the z-direction (see Fig. 1) the ellipse representing the polarization is determined by the angle ψ between the direction of the major axis and the x-direction (with $0 \leqslant \psi < \pi$) and by

$$\tan \chi = \pm \frac{b}{a} \qquad (b \leqslant a) \tag{1}$$

with the positive and negative sign for anticlockwise* and clockwise rotation respectively ($-\pi/4 \leqslant \chi \leqslant \pi/4$). Furthermore on the surface of a sphere of unit radius called the POINCARE sphere, each state of polarization is uniquely represented (see I) by a point P on the surface whose latitude and longitude are 2χ and 2ψ respectively. The cartesian co-ordinates s_1, s_2, s_3 of P, called the Stokes parameters, are

$$\mathbf{s} \equiv \begin{cases} s_1 = \cos 2\chi \cos 2\psi \\ s_2 = \cos 2\chi \sin 2\psi \\ s_3 = \sin 2\chi \end{cases} \tag{2}$$

and determine the polarization vector $\mathbf{s} \equiv (s_1, s_2, s_3)$. Thus in particular for linear polarization $s_3 = 0$ and for circular polarization $s_1 = 0$, $s_2 = 0$ and $s_3 = \pm 1$.

As was indicated in I, the evolution of the state of polarization for a plane electromagnetic wave propagating in the z-direction, in a medium whose optical properties only depend on z, is described by the following equation:

$$\frac{\mathrm{d}\mathbf{s}}{\mathrm{d}z} = \mathbf{\Omega}(z) \times \mathbf{s}(z) \tag{3}$$

where

$$\mathbf{\Omega} = \frac{\omega}{c}(\mu_1 - \mu_2)\mathbf{s}_{c2} \tag{4}$$

and ω is the wave frequency, μ_1 and μ_2 are the refractive indices of the slow and fast characteristic waves respectively, $\mathbf{s}_{c2}$ is the polarization vector of the fast characteristic wave.

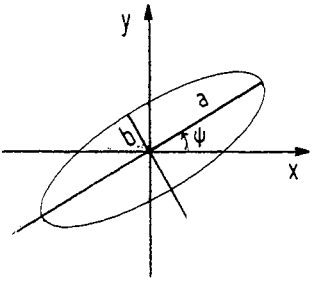

FIG. 1.—The polarization ellipse.

* For an observer looking towards the radiation source.

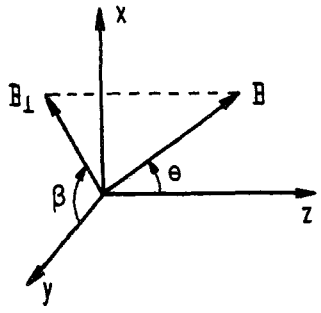

FIG. 2.—Magnetic field vector diagram.

It should be noted that the only requirement for the validity of (3) is that the radiation wavelength should be small compared to the scale length of gradients in the plasma. However in I we were interested in obtaining an analytical solution and this is only possible when $(\mu_1 - \mu_2) \ll 1$ (see Section 5). Therefore in giving the explicit expression of $\mathbf{\Omega}(z)$ for a plasma in a magnetic field the assumption $\omega \gg \omega_p$, the plasma frequency, was introduced. Since we now wish to use (3) for a numerical solution, we no longer need this assumption and we can write the exact expression of $\mathbf{\Omega}(z)$.

As in I let us indicate by θ the angle between $\mathbf{B}$ and $\mathbf{z}$ and by β the angle between $\mathbf{z} \times (\mathbf{B} \times \mathbf{z})$ and $\mathbf{y}$ (see Fig. 2). Then, neglecting collisions and ion motion, we have (see HEALD and WHARTON, 1965)

$$(\mu_{1,2})^2 = 1 - \frac{\omega_p^2}{\omega^2}\left\{1 - \frac{\omega_c^2}{\omega^2}\frac{\sin^2\theta}{2(1-\omega_p^2/\omega^2)} \pm \frac{\omega_c^2}{\omega^2}\frac{\sin^2\theta}{2(1-\omega_p^2/\omega^2)}[1+F^2]^{1/2}\right\}^{-1} \tag{5}$$

and

$$\tan\chi_2 = [(1+F^2)^{1/2} - 1]/F \tag{6}$$

$$\psi_2 = -\beta \tag{7}$$

where ω_c is the electron cyclotron frequency eB/mc and

$$F = \frac{2\omega}{\omega_c}\left(1 - \frac{\omega_p^2}{\omega^2}\right)\frac{\cos\theta}{\sin^2\theta} \tag{8}$$

and the subscripts 1 and 2 indicate quantities referring to the slow and fast characteristic waves respectively. Thus from equations (2), (6) and (7) we obtain*

$$\mathbf{s}_{c2} \equiv \begin{cases} \cos 2\beta(1+F^2)^{-1/2} \\ -\sin 2\beta(1+F^2)^{-1/2} \\ F(1+F^2)^{-1/2} \end{cases} \tag{9}$$

* In I the minus sign was accidentally omitted in the equation for the second component of $\mathbf{s}_{c2}$. However the results of that paper are not affected by this.

If B_x, B_y, B_z are the Cartesian components of **B** and if we call

$$N = \frac{\omega_p^2}{\omega^2} \tag{10}$$

$$D = 1 - \left(\frac{e}{\omega mc}\right)^2 \left[\frac{B_x^2 + B_y^2}{1-N} + B_z^2\right] \tag{11}$$

$$G = \frac{\omega_p^2}{2\omega^4}\left(\frac{e}{mc}\right)^2 \left[\frac{B_x^2 + B_y^2}{1-N}\right]\frac{1}{D} \tag{12}$$

then we can put (5) in the form

$$(\mu_{1,2})^2 = 1 - (N/D) + G \pm G(1+F^2)^{1/2} \tag{13}$$

and

$$\mu_1 - \mu_2 = \frac{\mu_1^2 - \mu_2^2}{(\mu_1 + \mu_2)} = \frac{G(1+F^2)^{1/2}2}{(\mu_1+\mu_2)}. \tag{14}$$

Finally introducing (9) and (14) into (4) we obtain

$$\mathbf{\Omega} \equiv \frac{\omega_p^2}{(\mu_1+\mu_2)c\omega^3 D} \times \begin{cases} \left(\frac{e}{mc}\right)^2 \left(\frac{B_y^2 - B_x^2}{1-N}\right) \\ -\left(\frac{e}{mc}\right)^2 \frac{2B_x B_y}{1-N} \\ 2\omega \frac{e}{mc} B_z \end{cases} \tag{15}$$

and $\mathbf{\Omega}$ depends on z through the quantities B_x, B_y, B_z and ω_p. This exact expression for $\mathbf{\Omega}$ reduces to the approximate one obtained in I if we put $N \ll 1$ and $\mu_1 + \mu_2 \simeq 2$.

3. PROPAGATION IN A TOKAMAK ALONG A VERTICAL CHORD. DIMENSIONLESS PARAMETERS AND PROPAGATION EQUATION

We will now apply the results of the previous section to the case of propagation in a Tokamak in a meridian plane (see Fig. 3) along a vertical chord.

If a is the minor radius of the plasma, let us introduce dimensionless variables $X = x/a$ and $Z = z/a$ and call $r = (X^2 + Z^2)^{1/2}$ the dimensionless distance from the centre. We will here assume that the plasma density n and the current density j only depend on r. Thus introducing the dimensionless functions $f(r)$, $b(r)$ we can write

$$n(r) = n_0 f(r) \tag{16}$$

where n_0 is the density at the centre; the poloidal magnetic field has a purely azimuthal component with magnitude in the cylindrical approximation

$$B_p(r) = (4\pi/rc)\int_0^r j(r')r'\,dr' \equiv B_I b(r) \tag{17}$$

where $B_I = B_p(1) = (2I/ac)$ and I is the toroidal plasma current. Thus

$$B_z = B_I b(r) X/r; \qquad B_x = -B_I b(r) Z/r. \tag{18}$$

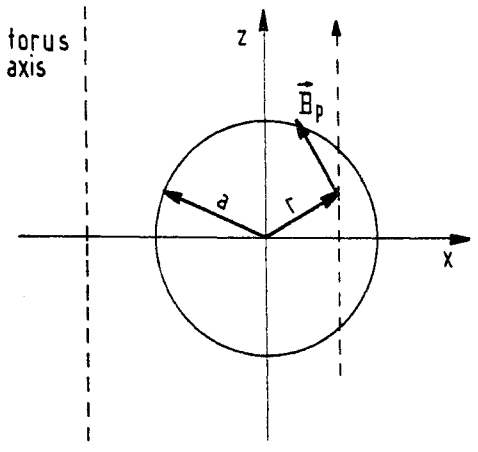

FIG. 3.—Co-ordinates in Tokamak meridian plane.

For a given value of X, we can put

$$B_x = B_I g(Z); \qquad B_z = B_I h(Z) \tag{19}$$

where

$$g(Z) = -bZ/r; \qquad h(Z) = bX/r \tag{20}$$

hence f and h are even functions of Z, while g is odd. Furthermore the toroidal field B_T does not depend on Z and

$$B_y = B_T. \tag{21}$$

In (19) and (21) both B_I and B_T can be positive or negative quantities and we can now write (3), which determines the evolution of the state of polarization, in the dimensionless form

$$\frac{\mathrm{d}\mathbf{s}}{\mathrm{d}Z} = \mathbf{T}(Z) \times \mathbf{s}(Z) \tag{22}$$

where $\mathbf{T} = a\boldsymbol{\Omega}$. Let us introduce the following dimensionless parameters, where ω_{p0} is the value of ω_p at $r = 0$,

$$\begin{cases} M = \dfrac{a\omega}{2c}\dfrac{\omega_{p0}^2}{\omega^4}\left(\dfrac{eB_T}{mc}\right)^2 \\ P = \dfrac{a\omega}{c}\dfrac{\omega_{p0}^2}{\omega^3}\dfrac{eB_I}{mc} \\ Q = B_T/B_I \\ N_0 = (\omega_{p0}/\omega)^2 \end{cases} \tag{23}$$

so that

$$U = \frac{eB_T}{\omega mc} = \frac{2M}{PQ}. \tag{24}$$

Thus from (15), using equations (19), (21) and (22) we obtain

$$\mathbf{T} \equiv \frac{2}{D(\mu_1+\mu_2)} \times \begin{cases} Mf(Z)\left\{\dfrac{1-[g(Z)/Q]^2}{1-N_0 f(Z)}\right\} \\ -\dfrac{M}{Q} f(Z)\left\{\dfrac{2g(Z)}{1-N_0 f(Z)}\right\} \\ Pf(Z)h(Z) \end{cases} \tag{25}$$

where μ_1 and μ_2 are given by (13) and from equations (8), (10), (11) and (12)

$$\begin{cases} N = N_0 f(z) \\ D = 1 - U^2\left\{\dfrac{1+[g(Z)/Q]^2}{1-N_0 f(Z)} + \left[\dfrac{h(Z)}{Q}\right]^2\right\} \\ G = \dfrac{N_0 U^2}{2D} f(Z)\left\{\dfrac{1+[g(Z)/Q]^2}{1-N_0 f(Z)}\right\} \\ F = \dfrac{P}{M} h(Z)\left\{\dfrac{1-N_0 f(Z)}{1+[g(Z)/Q]^2}\right\}. \end{cases} \tag{26}$$

We can now use the expression (25) of the components of $\mathbf{T}$ for the numerical integration of (22), which corresponds to the following system of three equations

$$\begin{cases} \dfrac{ds_1}{dZ} = T_2(Z)s_3(Z) - T_3(Z)s_2(Z) \\ \dfrac{ds_2}{dZ} = T_3(Z)s_1(Z) - T_1(Z)s_3(Z) \\ \dfrac{ds_3}{dZ} = T_1(Z)s_2(Z) - T_2(Z)s_1(Z). \end{cases} \tag{27}$$

Equations (22) or (27) imply $s^2 = {s_1}^2 + {s_2}^2 + {s_3}^2 = \text{const.} = 1$ so that it is possible to eliminate one variable and reduce the equations to two, however for a numerical integration it is convenient to retain the three variables, and to check the quality of the integration by verifying that $|s^2 - 1| \ll 1$. The integration starts at $Z = -Z_0 = -(1-X^2)^{1/2}$ where $\mathbf{s}$ has the initial value $\mathbf{s}_0 \equiv (s_{10}, s_{20}, s_{30})$, to be assigned, and it ends at $Z = +Z_0$ giving the output value of $\mathbf{s}$ (which is a function of X). This output value can then be used to determine all the quantities of interest of the transmitted radiation. In particular using equations (1) and (2) it can be shown that the ellipticity $\varepsilon = b/a$ is given by

$$\varepsilon = |s_3|/(1+[1-{s_3}^2]^{1/2}) \tag{28}$$

the orientation of the ellipse is

$$\psi = \tfrac{1}{2}\tan^{-1}(s_2/s_1) \tag{29}$$

the fraction P_n of the output radiation power in the polarization orthogonal* to

* We recall that two states of polarization $\mathbf{s}_a$ and $\mathbf{s}_b$ are orthogonal if $\mathbf{s}_a = -\mathbf{s}_b$. Thus if $\mathbf{s}_a$ is a linear polarization, $\mathbf{s}_b$ is the linear polarization perpendicular to the former; if $\mathbf{s}_a$ is circular polarization, $\mathbf{s}_b$, is again circular, rotating in the opposite direction.

the input polarization is

$$P_n(\mathbf{s}_0) = \tfrac{1}{2}[1 - s_1 s_{10} - s_2 s_{20} - s_3 s_{30}] = \tfrac{1}{2}[1 - \mathbf{s} \cdot \mathbf{s}_0] \tag{30}$$

P_n is the fraction of the output power transmitted through a polarizer crossed with the input polarization. Thus if $\mathbf{s} = \mathbf{s}_0$, $P_n = 0$. By considering the symmetry of the Poincaré sphere it is easily verified that, for two input polarizations which are orthogonal, P_n is the same, namely

$$P_n(\mathbf{s}_0) = P_n(-\mathbf{s}_0). \tag{31}$$

Apart from the profile functions $f(r)$, $b(r)$ and the initial polarization $\mathbf{s}_0$, the physical parameters which determine the solution are five: a, B_T, I, $\lambda = 2\pi c/\omega$ and n_0. An advantage of using a dimensionless analysis is that, as shown above, the independent dimensionless variables are only four, e.g. N_0, P, U, Q, whose values are given by the following expressions

$$\begin{aligned} N_0 &= 0.889 \times 10^{-13} \lambda^2 n_0 \\ P &= 1.036 \times 10^{-14} \lambda^2 n_0 I \\ U &= 0.934 \lambda B_T \\ Q &= 50 a B_T / I \end{aligned} \tag{32}$$

where λ and a are in cm, n_0 in cm^{-3}, I in kA, B_T in Tesla.

It should be emphasized that, as discussed in I, equation (3) i.e. equations (27) describe the process whereby for each infinitesimal slab $(Z, Z + \mathrm{d}Z)$, the wave is resolved into the two (local) characteristic waves, it is allowed to propagate through $\mathrm{d}Z$ considered to be uniform; the wave leaving the slab and entering the next one is again resolved into the new characteristic waves and so on. In the paper by Craig this same procedure is carried out explicitly, with the consequence that the algebra is more cumbersome and the numerical analysis becomes very lengthy if a good accuracy is required i.e. if the chord is to be divided into many intervals.

4. NUMERICAL RESULTS FOR DITE AND FOR FT

In order to compare with the calculations of Craig let us assume, as he does,

$$n = n_0(1 - r^2); \qquad j = j_0(1 - r^d). \tag{33}$$

Then from (16) and (17) we have

$$f = (1 - r^2) = (1 - X^2 - Z^2) \tag{34}$$

$$b(r) = [(d+2)r - 2r^{d+1}]/d. \tag{35}$$

Using the equations of Section 3, calculations have been carried out for different sets of parameters. It is found that, for a given input polarization $\mathbf{s}_0$, the output polarization $\mathbf{s}$ depends on the signs of both B_T and I; however P_n depends only on the sign of B_T.

For example with the parameters (appropriate to the DITE Tokamak at Culham) used by Craig, namely $a = 24$ cm, $I = \pm 200$ kA, $B_T = \pm 3$T, $\lambda = 1$ mm and neglecting the dependence of B_T on X, we obtain the curves of Fig. 4. These give P_n as a function of X for $d = 2$ and different values of n_0, for $B_T = 3$T and for

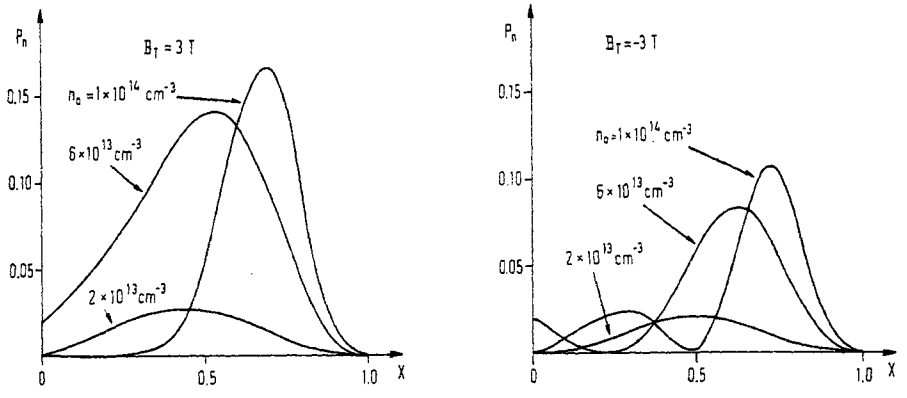

FIG. 4.—P_n vs X for $a = 24$ cm, $I = 200$ kA, $\lambda = 1$ mm, $d = 2$, $\mathbf{s}_0 \equiv (1, 0, 0)$.

$B_T = -3$T, when $\mathbf{s}_0 \equiv (1, 0, 0)$ i.e. the input wave is linearly polarized along the x-direction. It can be seen that the second set of curves coincides with those of Craig, whereas the first set is quite different. This difference tends to zero when P_n is small (e.g. when the density is small) and the analytical results of Section 5.1 hold. It can be shown analytically that the general fact that P_n does not depend on the sign of I is due to the symmetry of the functions $f(r)$, $b(r)$ whereby n, B_y and B_z are even functions of Z and B_x is odd. Furthermore the same P_n is obtained for input polarizations which are orthogonal (in particular for two perpendicular linear polarizations) as is required by (31).

The number of steps in the integration along the chord has been changed in order to check the quality of the calculation. Figure 5 compares the result of using 10 steps and 100 steps. Since in going from 100 to 200 steps the difference found is everywhere less than 1%, 100 steps were used in all the other calculations here reported.

Calculations for parameters appropriate to the FT Tokamak at Frascati have been made including the X dependence of B_T. If B_{T0} is the value on the toroidal axis and α is the ratio of minor to major radius, then

$$B_T = B_{T0}(1 + \alpha X)^{-1}. \tag{36}$$

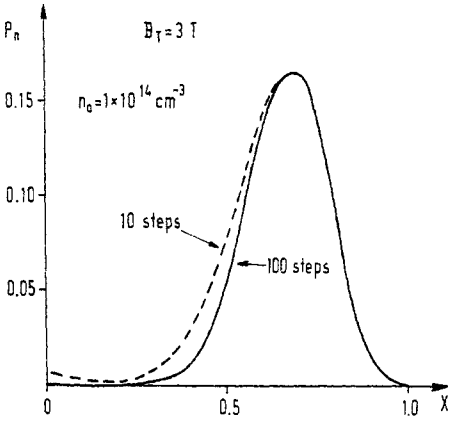

FIG. 5.—P_n vs X for parameters as in Fig. 4, for 10-step and 100-step calculations.

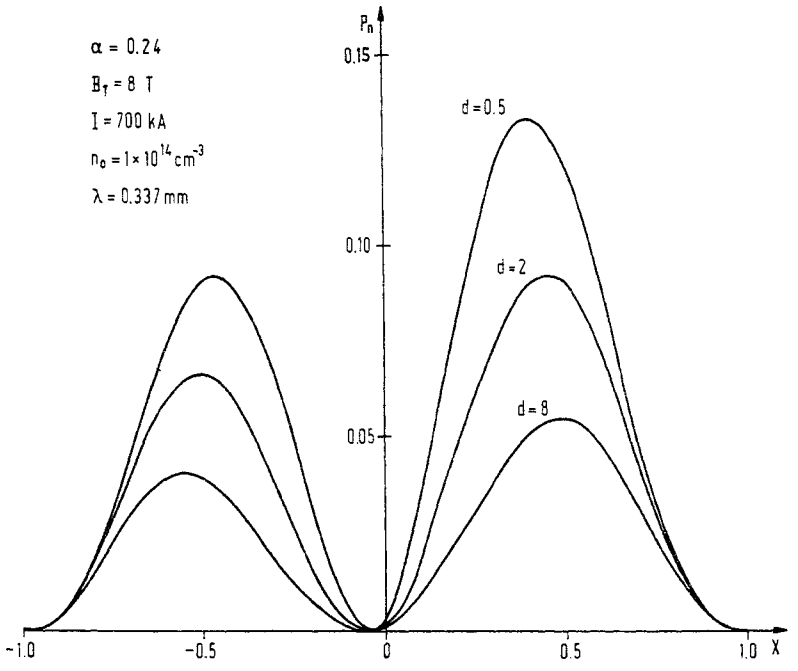

FIG. 6.—P_n vs X for $\mathbf{s}_0 \equiv (1, 0, 0)$, $\psi_0 = 0$, $a = 20$ cm.

For FT, $\alpha = 0.24$. Figure 6 shows P_n across a diameter for $\mathbf{s}_0 \equiv (1, 0, 0)$ for different current profiles ($d = 0.5$, 2 and 8) and other parameters as indicated. The wavelength used, $\lambda = 0.337$ mm, is short enough so that refraction due to transverse gradients can be negligible also at high density. Figure 7 shows the effect on P_n of a change of sign of B_T for $d = 2$. Again a change of sign of I has no effect on P_n. Figure 8 shows P_n for the same set of plasma parameters as Fig. 6 but with

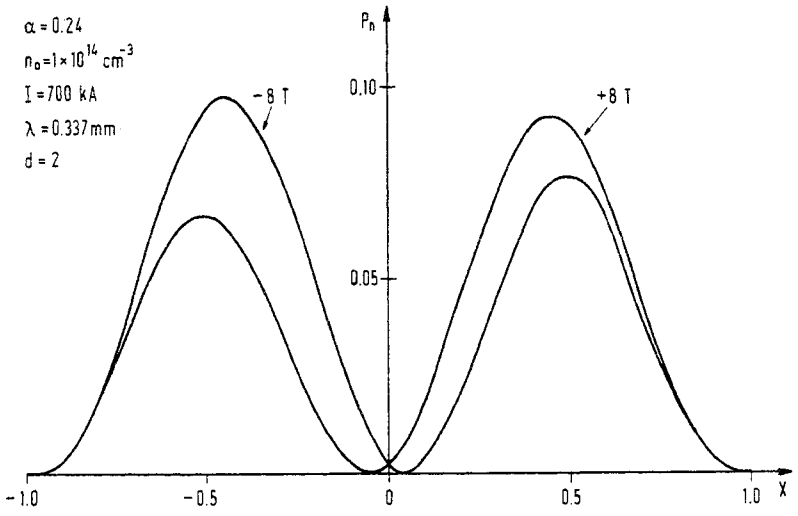

FIG. 7.—P_n vs X for $\mathbf{s}_0 \equiv (1, 0, 0)$, $\psi_0 = 0$, $a = 20$ cm.

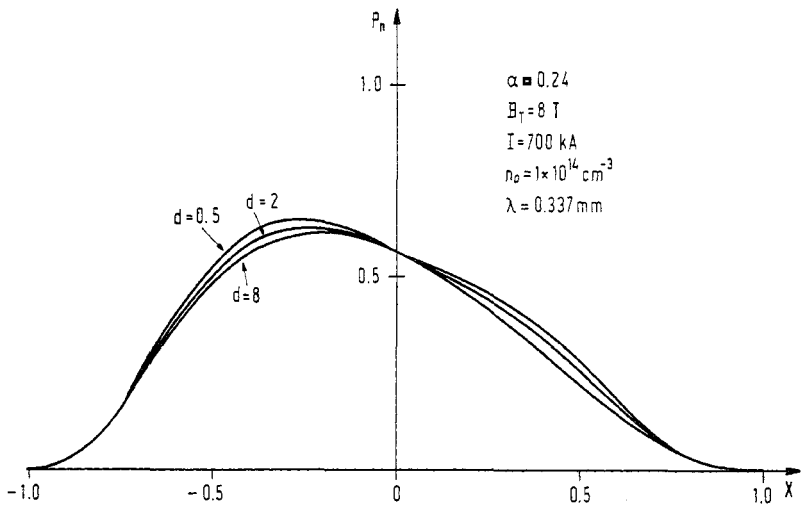

FIG. 8.—P_n vs X for $\mathbf{s}_0 \equiv (0, 1, 0)$, $\psi_0 = 45°$, $a = 20$ cm.

$\mathbf{s}_0 \equiv (0, 1, 0)$ i.e. linear polarization oriented at 45° to the x-direction. It can be seen that the curves are relatively insensitive to the value of d, i.e. to the current profiles and depend mainly on the density profile as will be discussed in Section 5.1. Such curves, as proposed by Craig, can be used to measure the density profile. Finally, Fig. 9 shows a plot of the orientation of the output ellipse, i.e. ψ given by (29), for the parameters of Fig. 6. This quantity can be determined accurately by using a rotating polarizer on the output and measuring the phase shift of the signal. It can be seen that the values of ψ are large compared with the values of P_n of Fig. 6, however the sensitivity to the current profile ($d = 0.5$ and 2)

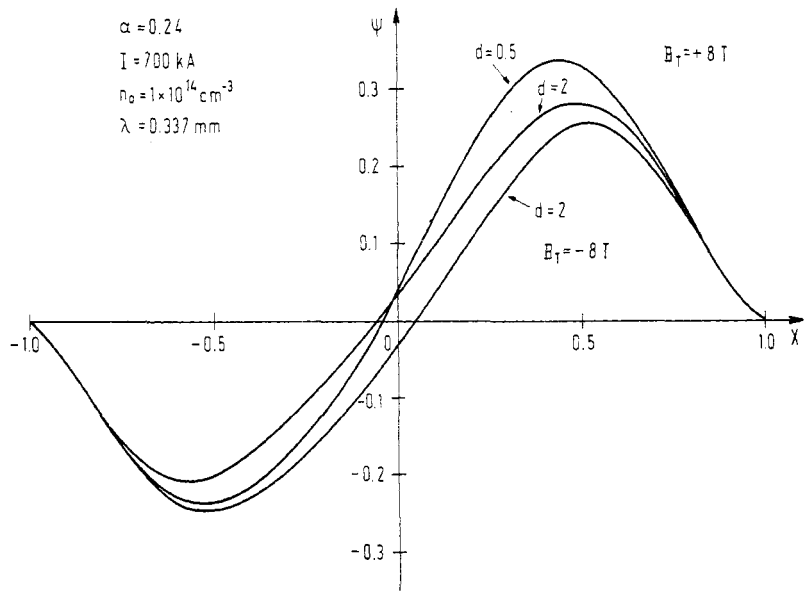

FIG. 9.—ψ vs X for $\mathbf{s}_0 \equiv (1, 0, 0)$, $\psi_0 = 0$, $a = 20$ cm.

is decreased. Again there is a polarity effect of B_T and a change of I to $-I$ changes ψ into $-\psi$.

If P_n or ψ are measured as functions of X, by making a best fit to the family of curves computed for different values of d, the nearest standard profile of j can be determined. In an experiment, where possibly one wishes to follow the profile evolution in time, many computed profiles will be required. In this case the numerical method of Section 3 should be particularly useful since it is simple and fast.

5. ANALYTIC SOLUTION GIVEN BY A SERIES

Let us put

$$w = \int_0^z \mathrm{d}z\, |\mathbf{\Omega}(z)|. \tag{37}$$

It can be shown (DE MARCO and SEGRE, 1977), that the solution of (3) can be given in the form of a series as follows

$$\mathbf{s}(z) = \mathbf{s}_0 + \mathbf{a}_0(z) + \sum_1^\infty \mathbf{a}_n(z) \tag{38}$$

where $\mathbf{s}_0$ is the initial value of $\mathbf{s}$ and

$$\mathbf{a}_0 = \int_0^z \mathrm{d}z \mathbf{\Omega} \times \mathbf{s}_0 \tag{39}$$

$$\mathbf{a}_n = \int_0^z \mathrm{d}z (\mathbf{\Omega} \times \mathbf{a}_{n-1}) \tag{40}$$

and one finds

$$|\mathbf{a}_n| \leqslant \frac{w^{n+1}}{(n+1)!}. \tag{41}$$

5.1. *Analytic solution for* $w \ll 1$

The series solution is very convenient if $w \ll 1$ since then, neglecting higher order terms, the approximate solution is

$$\mathbf{s}(Z) \simeq \mathbf{s}_0 + \mathbf{a}_0 \tag{42}$$

and the error E is

$$E \leqslant \sum_1^\infty |\mathbf{a}_n| \leqslant \sum_1^\infty w^{n+1}/(n+1)! = e^w - 1 - w. \tag{43}$$

Thus the output polarization for the propagation described in Section 3 is given by

$$\mathbf{s} \simeq \mathbf{s}_0 + \mathbf{W} \times \mathbf{s}_0 \tag{44}$$

where

$$\mathbf{W} = \int_{-z_0}^{z_0} \mathbf{T}(Z)\, \mathrm{d}Z \tag{45}$$

$|\mathbf{W}| \leqslant w$ and $\mathbf{T}(Z)$ is given by (25). Usually the condition $w \ll 1$ implies $(\omega_P/\omega)^2 \ll 1$ and $(\omega_c/\omega) \ll 1$ so that in the equations of Section 3 we have $(\mu_1 + \mu_2) \simeq 2$ and $D \simeq 1$ and so

$$\mathbf{W} \equiv \begin{cases} W_1 \simeq M \int_{-z_0}^{z_0} f(Z)\{1 - [g(Z)/Q]^2\}\, dZ \\ W_2 \simeq -2(M/Q) \int_{-z_0}^{z_0} f(Z) g(Z)\, dZ = 0. \\ W_3 \simeq P \int_{-z_0}^{z_0} f(Z) h(Z)\, dZ \end{cases} \tag{46}$$

Where $W_2 = 0$, because fg is an odd function of Z; $M \ll 1$, $P \ll 1$ are required. Equation (44) is the approximate solution which was used in I for a method to obtain $j(r)$ analytically. We can here use it (to a higher order) to derive a property of P_n which Craig found numerically. Let us consider a linearly polarized incident wave with an orientation ψ_0: so $s_{10} = \cos 2\psi_0$, $s_{20} = \sin 2\psi_0$, $s_{30} = 0$. Since, as will be apparent shortly, P_n has no linear term in $\mathbf{W}$, in order to evaluate P_n we must take also the second order term in $\mathbf{s}$, i.e.

$$\mathbf{s} \simeq \mathbf{s}_0 + \mathbf{W} \times \mathbf{s}_0 + \int_{-z_0}^{z_0} dZ \mathbf{T}(Z) \times \left[\int_{-z_0}^{z_0} dZ' \mathbf{T}(Z') \times \mathbf{s}_0 \right]. \tag{47}$$

Using this expression in (30) one finds

$$P_n = \tfrac{1}{2}(1 - \mathbf{s} \cdot \mathbf{s}_0) \simeq (W_3^2 + W_1^2 \sin^2 2\psi_0)/4. \tag{48}$$

When $\psi_0 = 0$ or $\psi_0 = \pi/2$, $P_n \simeq W_3^2/4$ and the expression (46) for W_3 shows that, for a given density profile $f(Z)$, P_n depends on the current density distribution through $h(Z)$. The analytic procedure to invert $[P_n(X)]^{1/2}$ in order to obtain $j(r)$ is discussed in I.

When $\psi_0 = \pm \pi/4$, $P_n = (W_3^2 + W_1^2)/4$ and if

$$W_1^2 \gg W_3^2 \tag{49}$$

we have $P_n \simeq W_1^2/4$. For a Tokamak $Q^2 = (B_T/B_I)^2 \gg 1$ and so

$$W_1 \simeq M \int_{-z_0}^{z_0} f(Z)\, dZ. \tag{50}$$

Thus, for $\psi_0 = \pm \pi/4$, P_n only depends on the density profile, confirming Craig's numerical result and an Abel inversion of $[P_n(X)]^{1/2}$ gives the density profile $f(r)$. Since the order of magnitude of W_1 is M and that of W_3 is P, the condition (49) implies

$$(M/P)^2 = \left(\frac{eB_T}{2\omega mc} \frac{B_T}{B_I} \right)^2 \gg 1 \tag{51}$$

or

$$(M/P)^2 = [23.4 \lambda a B_T^2 / I]^2 \gg 1 \tag{52}$$

where the units are the same as in (32).

Also in the case where a numerical evaluation of P_n is made for a best fit determination of $f(r)$ and $b(r)$, condition (51) ensures a weak dependence of P_n on $b(r)$ for $\psi_0 = \pm \pi/4$. When the condition is not satisfied, for $\psi_0 = \pm \pi/4$ we have $P_n \simeq (W_3^2 + W_1^2)/4$ and the f dependence does not separate out. However, since the difference of the output powers for $\psi_0 = 0$ or $\pi/2$ and for $\psi_0 = \pm \pi/4$ is

$$\Delta P \equiv P_n(\pi/4 \quad \text{or} \quad -\pi/4) - P_n(\pi/2 \quad \text{or} \quad 0) = W_1^2/4$$

a measurement of ΔP can be used to determine the density profile.

6. CONCLUSIONS

The change of polarization of an electromagnetic wave propagating along vertical chords of a Tokamak can be used to determine the poloidal field.

A simple numerical method is derived which gives the output polarization as a function of plasma parameters. One obtains the output polarization vector $\mathbf{s} = (s_1, s_2, s_3)$ by a numerical integration of equations (27) (where T_1, T_2, T_3 depend on plasma parameters as indicated by equations (23)–(26)) from the initial value $\mathbf{s}_0$ at $Z = -Z_0$, up to $Z = +Z_0$. This method has been used to show that the output polarization in general depends on the sign of the toroidal and poloidal magnetic fields, and to obtain typical values for parameters of present devices.

Using an exact solution in the form of a series it is shown that with an input polarization which is linear and at 45° to the toroidal field the electron density can be determined and this becomes especially simple when condition (52) is satisfied. With an input polarization at 0° or 90° to the toroidal field the product of poloidal field and electron density can be determined.

The numerical method derived is very simple and should be particularly useful in the analysis of future experimental results, where many calculations will be required if a procedure of fitting to trial functions is used.

REFERENCES

CRAIG A. D. (1976) *Plasma Phys.* **18,** 777.
DE MARCO F. and SEGRE S. E. (1972) *Plasma Phys.* **14,** 245.
DE MARCO F. and SEGRE S. E. (1977) *Opt. Commun.* **23,** 125.
HEALD M. A. and WHARTON C. B. (1965) *Plasma Diagnostics with Microwaves,* Wiley, New York.